INTRODUCING ANNIE: A SIMPLE THREE-PARAMETER ANISOTROPIC VELOCITY MODEL FOR SHALES

MICHAEL SCHOENBERG[1*], FRANCIS MUIR[2] and COLIN SAYERS[1]

[1] *Schlumberger Cambridge Research, Madingley Rd., Cambridge CB3 0EL, U.K.*
[2] *Department of Geophysics, Stanford University, Stanford, CA 94305-2215, U.S.A.*
[*] *present address: Schlumberger-Doll Research, Ridgefield, Connecticut 06877-4108, U.S.A.*

(Received July 10, 1995; revised version accepted October 24, 1995)

ABSTRACT

Schoenberg, M., Muir, F. and Sayers, C., 1996. Introducing ANNIE: a simple three-parameter anisotropic velocity model for shales. *Journal of Seismic Exploration*, 5: 35-49.

A simple three-parameter transversely isotropic (TI) model is presented as a reasonable first approximation for the elastic behavior of a wide variety of shales. The model has the property that the zero-offset normal-moveout velocity is equal to the vertical velocity, a condition often approached by many shales. This constraint reduces the number of independent parameters to four. Under this assumption, a simple accurate approximation to the P-phase slowness surface may be found from which all oblique P-wave slownesses are predictable from just two speeds, the zero-offset normal-moveout velocity and the horizontal velocity. When seismic exploration data is confined to compressional waves recorded in a rather narrow aperture, such a TI medium will 'appear isotropic'. A further constraint on the model parameters, reducing the number of independent parameters to three, connects the behavior in the horizontal plane to the behavior in the vertical plane. It allows for a generalization of the Lamé parameters to the case where the TI anisotropy is due solely to the existence of two shear moduli, one vertical, the other horizontal. These simple models for shales behave as a TI medium equivalent to an isotropic medium stiffened by the inclusion of horizontally bedded thin rigid plates.

KEY WORDS: seismic anisotropy, shales, anisotropic velocity analysis.

0963-0651/96/$5.00

INTRODUCTION

A simple three-parameter transversely isotropic (TI) velocity model, called ANNIE, is proposed as a reasonable first approximation for the elastic behavior of a wide variety of shales. Shales constitute a major component of sedimentary basins and play an important role in fluid flow and seismic wave propagation because of their low permeability and anisotropic microstructure. Under a microscope, they appear as stacks of more or less horizontally aligned platelets piled irregularly upon one another (Swan et al., 1989; Hornby et al., 1994), see Fig. 1. Despite this complexity, there is a characteristic shape of the phase-slowness surface for shales (Carrion et al., 1992; Dellinger et al., 1993; Sayers, 1994; Schoenberg, 1994), an example being the phase slowness surface for Greenhorn shale (Jones and Wang, 1981) which is compared in Fig. 2 with an elliptically anisotropic medium having the same axial P- and S-velocities. It is convenient to denote by c_{ij} the *density-normalized* elastic stiffness moduli in the 6×6 condensed notation. The horizontal P slowness $\sqrt{(1/c_{11})}$ is seen to be smaller than the vertical P slowness $\sqrt{(1/c_{33})}$. The qP-wave slowness curve bulges out from the ellipse connecting the vertical and horizontal P slownesses.

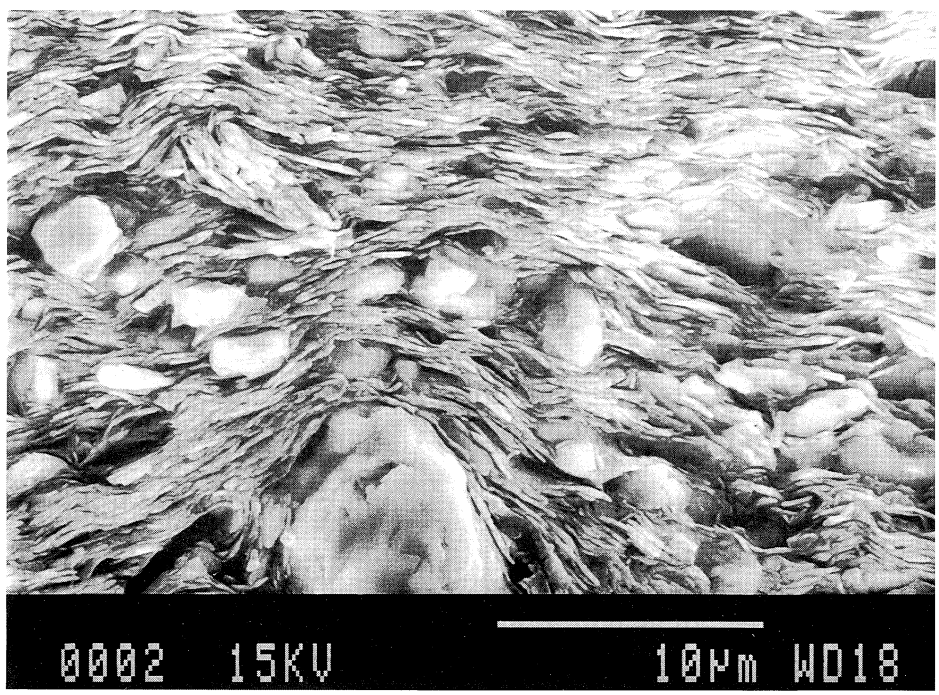

Fig. 1. Scanning electron micrograph of a shale from the Kimmeridge Clay formation, in Dorset, UK. Photograph by John Cook, Schlumberger Cambridge Research.

This is called 'positive anellipticity', and implies that for oblique directions the medium is slower (for qP-waves) than an elliptical TI medium with the same values of c_{11} and c_{33}. Positive anellipticity also implies that the qSV-phase slowness curve is pushed inwards from the circle that connects its horizontal and vertical slownesses, both of which are equal to $\sqrt{(1/c_{55})}$. For shales, this contraction between horizontal and vertical is sometimes enough for the qSV curve to have a slight concavity about an oblique direction corresponding to a small triplication in the wavefront, or group velocity curve. The SH slowness curve is always an ellipse, implying that the wavefront curve is elliptical as well, and for shales, typically, the horizontal SH slowness is smaller than the vertical shear slowness.

A further important observation is that while depths calculated from S-wave stacking velocities almost always exceed actual depths, sometimes by as much as 25%, depths calculated from P-wave stacking velocities are almost always within 10% of actual depths (Winterstein, 1986), and often much closer. It is because of this that isotropic analysis has been very successful for the seismic industry, as long as the total angular aperture has been relatively small (Winterstein, 1986). For a transversely isotropic medium, the P-wave normal-moveout velocity is given by

$$v^2_{NMOP} = c_{33} + (c_{13}+c_{33})(c_{13}+2c_{55}-c_{33}) / (c_{33}-c_{55}) \equiv c_{33}[1+2\delta^T] \quad , \quad (1)$$

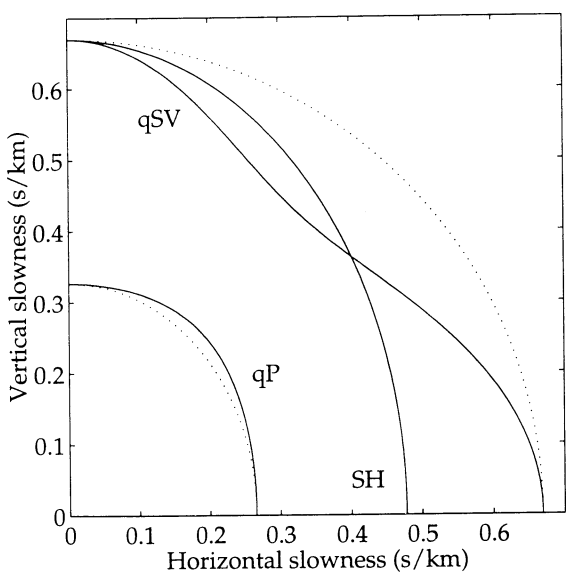

Fig. 2. Phase slowness curves for Greenhorn shale computed using the elastic stiffnesses measured at a confining stress of 0.1 MPa by Jones and Wang (1981). The dotted curves show the phase slowness curves for an elliptically anisotropic medium having the same axial P and S velocities.

where δ^T is one of Thomsen's anisotropy parameters, the one which is essentially the dimensionless difference between the normal moveout and vertical velocities (Thomsen, 1986). Since shales are the major source of transverse isotropy in sedimentary basins, it is to be expected that for such shales, δ^T, and hence, $c_{33}-c_{13}-2c_{55}$, is usually small. For example, the elastic stiffnesses, ρc_{ij}, in GPa found for Greenhorn shale at a confining stress of 0.1MPa (Jones and Wang, 1981) are as follows:

ρc_{11}	ρc_{33}	ρc_{55}	ρc_{66}	ρc_{13}	ρc_{12}	$\rho(c_{13} + 2c_{55} - c_{33})$
34.3	22.7	5.4	10.6	10.7	13.1	−1.2

and from these values, $\delta^T = -0.051$.

Another purpose of this note is to show that ANNIE belongs to a class of media which may be called 'plate stiffened', in that its anisotropic properties are the same as plate reinforced media in an isotropic background in the long wavelength limit. It will be seen that all such plate stiffened media satisfy the condition that $c_{13} + 2c_{55} - c_{33} = 0$, which is suggestive that in some sense shales can be thought of as a plate stiffened composite medium. In this regard observe the partially aligned platelets typical of shales shown in Fig. 1.

As an aside, the model described immediately below has been known as ANNIE, for better or worse, over the last twenty years; we feel it is expeditious to continue this somewhat whimsical nomenclature.

ANNIE - A SIMPLE MODEL FOR SHALES

ANNIE is a three parameter family of TI media specified by a 6×6 density-normalized elastic stiffness matrix, in condensed notation, of the form,

$$\mathbf{c} = \begin{bmatrix} \lambda+2\mu_H & \lambda & \lambda & 0 & 0 & 0 \\ \lambda & \lambda+2\mu_H & \lambda & 0 & 0 & 0 \\ \lambda & \lambda & \lambda+2\mu & 0 & 0 & 0 \\ 0 & 0 & 0 & \mu & 0 & 0 \\ 0 & 0 & 0 & 0 & \mu & 0 \\ 0 & 0 & 0 & 0 & 0 & \mu_H \end{bmatrix} , \qquad (2)$$

subject to

$$K_1 \equiv (\mu_H - \mu)/\mu > 0 \quad \text{and} \quad 0 < \gamma \equiv \mu/(\lambda+2\mu) \leq 1/2 \quad . \qquad (3)$$

Note that the parameters μ, μ_H and λ are of dimension [velocity^2] because of the density-normalization. The deviation from isotropy is due only to the non-zero

value of K_1. The parameter γ is the square of the ratio of the vertical S-wave velocity to the vertical P-wave velocity and is analogous to the square of the shear speed to compressional speed for isotropic media which is less than or equal to 1/2 when the dynamic Poisson's ratio is non-negative.

As this is a three parameter model for transverse isotropy, there are two constraints, in the form of strict equalities, on the set of five ordinarily independent TI parameters. The first constraint is that,

$$c_{13} + 2c_{55} - c_{33} = 0 \quad , \tag{4}$$

which, as discussed above, is equivalent to the vanishing of Thomsen's parameter δ^T. Thus ANNIE's zero offset normal moveout velocity is equal to its vertical velocity.

The second constraint is that

$$c_{13} = c_{12} \equiv c_{11} - 2c_{66} \quad , \tag{5}$$

which is also observed to be approximately true in many shales. This ties the SH-wave behavior to the qP,qS-wave behavior in that this constraint is equivalent to $c_{66}-c_{55} = (c_{11}-c_{33})/2$.

As this is a three-parameter model, two dimensionless parameters control the 'shape' of the elastic behavior of an ANNIE medium, K_1 and γ as defined in (3). All other dimensionless parameters can be defined in terms of these two. Thus, the other Thomsen parameters, ϵ^T and γ^T, are given by γ K_1 and K_1 /2, respectively. A more symmetric parameterization, for example in Carrion et al. (1992), gives,

$$\begin{aligned} \epsilon_P &= (c_{11}-c_{33})/(c_{11}+c_{33}) = \gamma K_1/(1+\gamma K_1) \quad , \\ \epsilon_S &= (c_{66}-c_{55})/(c_{66}+c_{55}) = (K_1/2)/(1+K_1/2) \quad , \end{aligned} \tag{6}$$

and anellipticity,

$$\begin{aligned} \epsilon_A &= [(c_{11}-c_{55})(c_{33}-c_{55}) - (c_{13}+c_{55})^2]/(c_{11}-c_{55})(c_{33}-c_{55}) \\ &= [2\gamma K_1/(1-\gamma)]/[1+2\gamma K_1/(1-\gamma)] = 4\epsilon_P\epsilon_S/(2\epsilon_S-\epsilon_P+3\epsilon_P\epsilon_S) \quad . \end{aligned}$$

An attractive feature of this parameterization is that all three of these parameters, ϵ_P, ϵ_S and ϵ_A are between 0 and 1.

qP MODELING

ANNIE can now be used to model shale regions. Of paramount interest for velocity analysis and tomography is the qP slowness relation which, for an ANNIE medium, can be very closely approximated by a simple approximate slowness relation that retains ANNIE's vertical and horizontal P-wave velocities and ANNIE's critical property that its zero-offset normal moveout P-wave velocity is equal to its vertical P-wave velocity. The advantage of the approximation, in addition to its simple form, is that it depends on only two parameters, the vertical and horizontal P-wave speeds,

$$\alpha = \sqrt{(\lambda + 2\mu)} \qquad \text{and} \qquad \alpha_H = \sqrt{(\lambda + 2\mu_H)} \quad ,$$

respectively, and not on shear wave speed $\beta = \sqrt{\mu}$.

The exact qP-qSV slowness relation for ANNIE in terms of α^2, α_H^2 and β^2 may be solved exactly for p_z^2, the vertical slowness squared, in terms of p_x^2, the horizontal slowness squared. The smaller root, the qP slowness relation, is given by

$$p_z^2 = (1/2\alpha^2\beta^2)[\alpha^2 + \beta^2 - (2\beta^2+\Delta\alpha_H^2)(1-\Delta)\alpha_H^2 p_x^2$$

$$- \sqrt{\{(\alpha^2 - \beta^2 - \Delta\alpha^2\alpha_H^2 p_x^2)^2 + 4\Delta(\alpha^2 - \beta^2)\beta^2\alpha^2\alpha_H^2 p_x^4\}}] \quad , \qquad (7)$$

where

$$\Delta \equiv (\alpha_H^2 - \alpha^2)/\alpha_H^2 = 2K_1\gamma \,/\, (1+2K_1\gamma) \quad .$$

Expanding the square root in powers of Δ and retaining only terms up to first order in Δ yields an approximate qP dispersion relation,

$$\alpha^2 p_z^2 \approx (1 - \alpha_H^2 p_x^2)(1 + \Delta\alpha_H^2 p_x^2) \quad , \qquad (8)$$

which is independent of β^2, which has the correct curvature at $p_x = 0$ and which yields the correct value of p_x when $p_z = 0$. Note that in the limit as $\beta^2 \to 0$, the exact root (7) becomes $\alpha^2 p_z^2 = (1 - \alpha_H^2 p_x^2)/(1 - \Delta\alpha_H^2 p_x^2)$, which is similar in form to our approximate expression (8) but more complicated to apply due to the division by a factor which vanishes along the real slowness axis in the post-critical regime.

Fig. 3 shows the qP phase slowness sheets for five different ANNIE models. They all have $\alpha_H^2 = 16$ and $\alpha^2 = 12$, i.e., $\Delta = 1/4$, but $\gamma = \beta^2/\alpha^2$ takes the values 0.1, 0.2, 0.3, 0.4, 0.5. The solid lines (almost overlaying one another) are the exact qP slowness sheets (7) and we see how invariant these sheets are to large changes in the value of β^2, and how good the approximation (the barely visible dashed line) is at this high level of anisotropy. It is instructive to consider the difference between the qP slowness relation and the circular P

slowness relation of an isotropic medium with P-wave velocity equal to α, the TI medium's vertical velocity. To do this note that from the approximate slowness curve recast in polar coordinates, $p = \sqrt{(p_x^2 + p_z^2)}$ and $\theta = \arctan(p_x/p_z)$, where θ is the angle measured from the vertical,

$$1/\alpha^2 p^2 = (1/2)[1 + \sqrt{\{1+4\{\Delta/(1-\Delta)^2\}\sin^4\theta\}}] \approx 1 + \{\Delta/(1-\Delta)\}\sin^4\theta \quad ,$$

to first order in Δ after imposing the correct value at $\theta = \pi/2$. For the isotropic medium,

$$1/\alpha^2 p^2 = 1 \quad .$$

Thus the difference,

$$\alpha p|_{\text{isotropic}} - \alpha p|_{\text{ANNIE}} \approx (\Delta/2)\sin^4\theta \approx \{(\alpha_H - \alpha)/\alpha_H\}\sin^4\theta \quad , \qquad (9)$$

to first order in $(\alpha_H - \alpha)/\alpha_H$ (again imposing the correct value at $\theta = \pi/2$). Thus for angles up to 30° or so from vertical, ANNIE's slowness curve is almost circular, and seismic P-wave experiments over such a medium would show little effect of the anisotropy within such an angular range.

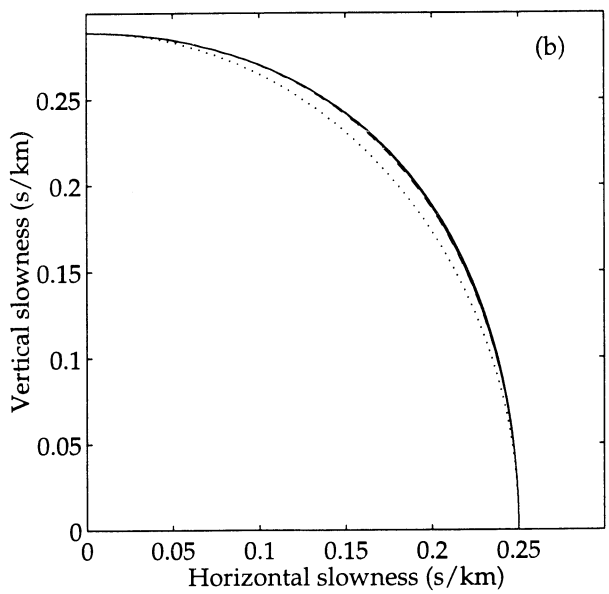

Fig. 3. qP phase slowness sheets for five different ANNIE models, all with $\alpha_H^2 = 16$ and $\alpha^2 = 12$, i.e., with dimensionless parameter $\Delta = 1/4$, but with $\beta^2/\alpha^2 = 0.1, 0.2, 0.3, 0.4, 0.5$. The dark solid lines are the exact results for these cases, and the fact that they overlay so well is an indication that the qP curves for ANNIE models are almost independent of β. The barely visible dashed line is the approximate qP slowness sheet, from (8). The dotted curve is the phase slowness curve for an elliptically anisotropic medium having the same axial P and S velocities as the ANNIE models.

BEST FITTING ANNIE MODEL FOR A GIVEN TI MEDIUM

To find the closest ANNIE model to a given TI medium, following Schoenberg and Douma (1988), we minimize the following expression in the three ANNIE parameters:

$$e^2 = (1/5) \sum_{11,33,55,66,13} [1-(c_{ij}^{ANNIE}/c_{ij})]^2 \quad ,$$

where c_{ij} and c_{ij}^{ANNIE} are the elastic stiffnesses of the anisotropic medium and best-fitting ANNIE model, respectively. This gives

$$(4c_{55}^2 + c_{33}^2)\mu + 2\, c_{55}^2\lambda = (2c_{55} + c_{33})c_{33}c_{55}$$

$$(4c_{66}^2 + c_{11}^2)\mu_H + 2c_{66}^2\lambda = (2c_{66} + c_{11})c_{11}c_{66}$$

$$2c_{11}^2c_{13}^2\mu + 2c_{33}^2c_{13}^2\mu_H + (c_{11}^2c_{33}^2 + c_{11}^2c_{13}^2 + c_{33}^2c_{13}^2)\lambda$$

$$= (c_{11}c_{33} + c_{11}c_{13} + c_{33}c_{13})c_{11}c_{33}c_{13} \quad .$$

The solution of these linear equations is:

$$\lambda = c_{13}[1 + (c_{13}/D)\{(c_{12}-c_{13})(4c_{55}^2 + c_{33}^2) + (c_{33}-c_{13}-2c_{55})(4c_{66}^2 + c_{11}^2)\}]$$

$$\mu_H = c_{66}[1 + (2c_{66}/D)\{(c_{12}-c_{13})(4c_{55}^2 + c_{33}^2 + c_{13}^2) - (c_{33}-c_{13}-2c_{55})c_{13}^2\}]$$

$$\mu = c_{55}[1 + (2c_{55}/D)\{(c_{33}-c_{13}-2c_{55})(4c_{66}^2 + c_{11}^2 + c_{13}^2) - (c_{12}-c_{13})c_{13}^2\}]$$

where

$$D = (4c_{55}^2 + c_{33}^2)(4c_{66}^2 + c_{11}^2) + c_{13}^2[(4c_{55}^2 + c_{33}^2) + (4c_{66}^2 + c_{11}^2)] \quad .$$

As an example, Hornby (1994) has measured ultrasonic wave velocities and calculated the elastic stiffnesses in two shales of Jurassic age as a function of confining stress. Fig. 4 compares these elastic stiffnesses with the best fitting ANNIE model. The agreement is seen to be reasonable, although the predicted values of c_{33} are somewhat too high. Fig. 5 compares the elastic stiffnesses measured by Vernik and Nur (1992) for a mature kerogen-rich shale containing bedding-parallel microcracks caused by the process of hydrocarbon generation with a fit to ANNIE. Finally, Johnston and Christensen (1995) have measured elastic stiffnesses for shales collected from three Devonian-Mississippian black shale formations. Fig. 6 compares the measurements for the four samples of New Albany shale of the Illinois Basin with a fit to ANNIE.

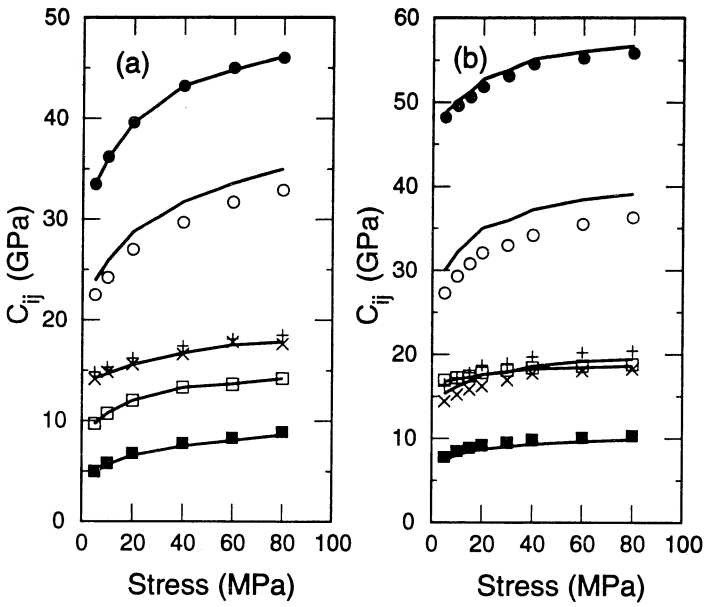

Fig. 4. Elastic stiffnesses C_{11} (•), C_{33} (○), C_{12} (×), C_{13} (+), C_{55} (■) and C_{66} (□) of two shales of Jurassic age measured by Hornby (1994) compared with the best fitting ANNIE models (solid curves).

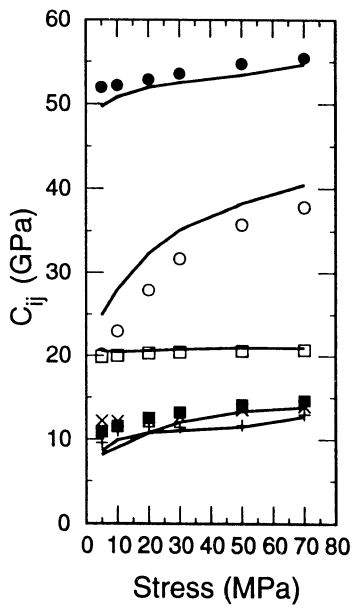

Fig. 5. Elastic stiffnesses C_{11} (•), C_{33} (○), C_{12} (×), C_{13} (+), C_{55} (■) and C_{66} (□) for a sample of mature kerogen-rich shale with bedding parallel cracks studied by Vernik (1993) compared with the best fitting ANNIE model (solid curves).

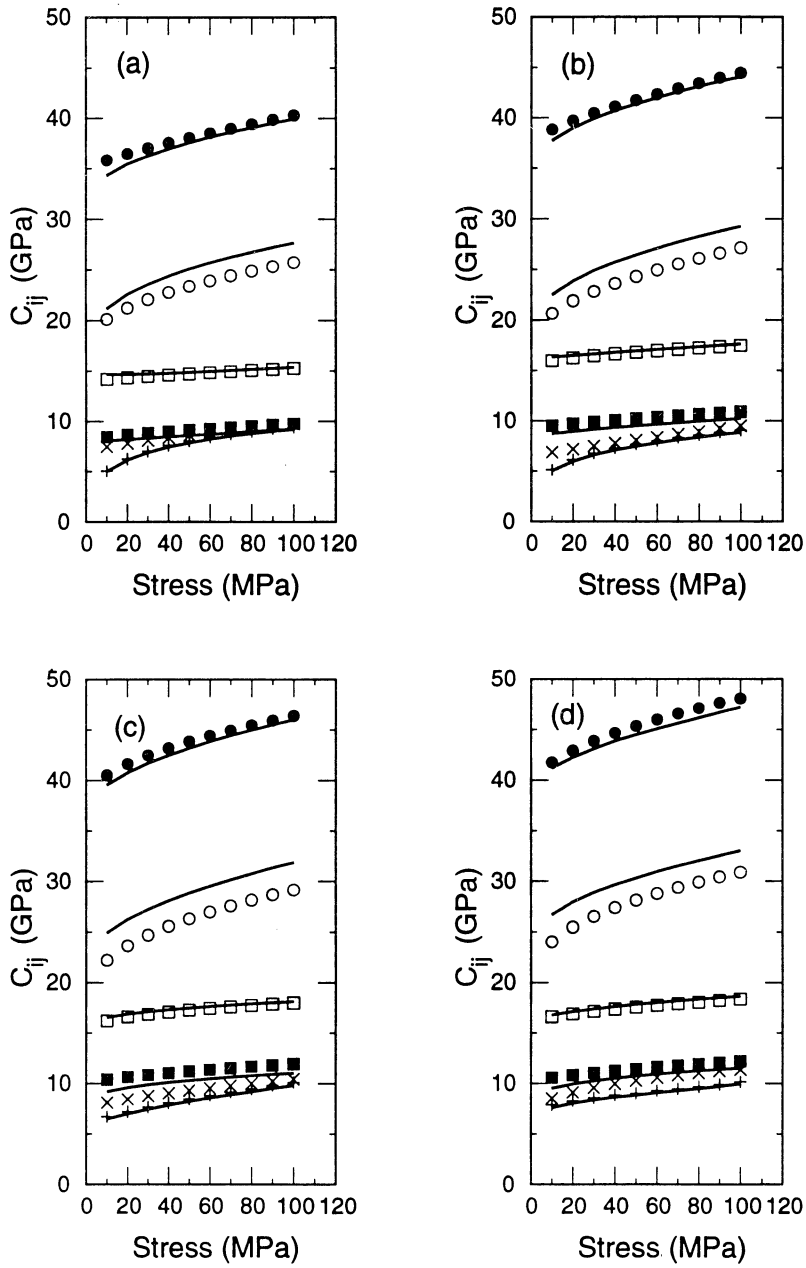

Fig. 6. Elastic stiffnesses C_{11} (•), C_{33} (○), C_{12} (×), C_{13} (+), C_{55} (■) and C_{66} (□) of four samples of shale from the New Albany shale of the Illinois basin compared with the best fitting ANNIE models (solid curves).

THIN RIGID PLATE STIFFENED MEDIA

The properties of plate stiffened media may be conveniently approached through the group formalism of Schoenberg and Muir (1989). We are looking for the long wavelength equivalent medium properties of a mixture of two layer constituents. Remembering that a group element corresponds to a total thickness of a particular constituent contained in a representative mixed layer of thickness H (and here we are letting the x_3-axis be perpendicular to the layering), let the first constituent be a background medium, denoted by subscript b, of total thickness (1-h)H, $0 \leq h \ll 1$, of density ρ_b and (in 6×6 condensed notation) with stiffness matrix $\mathbf{C}_b$ or equivalently, with compliance matrix $\mathbf{S}_b \equiv \mathbf{C}_b^{-1}$, so that

$$\mathbf{g}_b = \begin{bmatrix} (1-h)H \\ (1-h)H\rho_b \\ (1-h)H\mathbf{C}_{NNb}^{-1} \\ (1-h)H\mathbf{C}_{TNb}\mathbf{C}_{NNb}^{-1} \\ (1-h)H[\mathbf{C}_{TTb}-\mathbf{C}_{TNb}\mathbf{C}_{NNb}^{-1}\mathbf{C}_{NTb}] \end{bmatrix} = \begin{bmatrix} (1-h)H \\ (1-h)H\rho_b \\ (1-h)H[\mathbf{S}_{NNb}-\mathbf{S}_{NTb}\mathbf{S}_{TTb}^{-1}\mathbf{S}_{TNb}] \\ -(1-h)H\mathbf{S}_{TTb}^{-1}\mathbf{S}_{TNb} \\ (1-h)H\mathbf{S}_{TTb}^{-1} \end{bmatrix} . \quad (10)$$

Note that subscripts NN, TT, NT and TN refer to 3×3 submatrices of the original 6×6 matrix. In particular, in terms now only of subscripts, with the 3-axis normal to the layering,

$$NN = \begin{bmatrix} 33 & 34 & 35 \\ 43 & 44 & 45 \\ 53 & 54 & 55 \end{bmatrix} \quad TT = \begin{bmatrix} 11 & 12 & 16 \\ 21 & 22 & 26 \\ 61 & 62 & 66 \end{bmatrix} \quad TN = \begin{bmatrix} 13 & 14 & 15 \\ 23 & 24 & 25 \\ 63 & 64 & 65 \end{bmatrix} = NT^t$$

where superscript t denotes the transpose. Let the second constituent occupy thickness hH and, for it to be very rigid and dense, let its mass per unit area (in the plane of the layering) be $\hat{\rho}/h$ and its 6×6 compliance matrix be $h\hat{\mathbf{S}}$. Note that

$$(h\hat{\mathbf{S}})^{-1} = (1/h)\hat{\mathbf{S}}^{-1} \equiv (1/h)\hat{\mathbf{C}} \quad .$$

The group element of this second constituent in terms of the submatrices of the compliance matrix as $h \to 0$ is given by

$$\mathbf{g}_{st} = \begin{bmatrix} hH \\ H\hat{\rho} \\ h^2H[\hat{\mathbf{S}}_{NN}-\hat{\mathbf{S}}_{NT}\hat{\mathbf{S}}_{TT}^{-1}\hat{\mathbf{S}}_{TN}] \\ -hH\hat{\mathbf{S}}_{TT}^{-1}\hat{\mathbf{S}}_{TN} \\ H\hat{\mathbf{S}}_{TT}^{-1} \end{bmatrix} \quad . \quad (11)$$

Now, the key motivation of this group formalism is that the properties of the new homogeneous long wavelength equivalent medium are found by simple addition of the group elements of the constituents. Thus, the group element for infinitely thin stiffening layers interspersed in the background medium is given by adding group elements (10) and (11) and taking the limit as $h \to 0$. This yields

$$\mathbf{g} = \lim_{h\to 0}(\mathbf{g}_b + \mathbf{g}_{st}) = \begin{bmatrix} H \\ H(\rho_b + \hat{\rho}) \\ H\mathbf{C}_{NNb}^{-1} \\ H\mathbf{C}_{TNb}\mathbf{C}_{NNb}^{-1} \\ H[\mathbf{C}_{TTb} + \hat{\mathbf{S}}_{TT}^{-1} - \mathbf{C}_{TNb}\mathbf{C}_{NNb}^{-1}\mathbf{C}_{NTb}] \end{bmatrix} , \qquad (12)$$

from which we can see that the plate stiffened medium has density $\rho_b + \hat{\rho}$ and stiffness submatrices, $\mathbf{C}_{NNb}$, $\mathbf{C}_{TNb}$ (unchanged from the background) and $\mathbf{C}_{TTb} + \hat{\mathbf{S}}_{TT}^{-1}$, where

$$\hat{\mathbf{S}}_{TT}^{-1} = \begin{bmatrix} \hat{S}_{11} & \hat{S}_{12} & \hat{S}_{16} \\ \hat{S}_{12} & \hat{S}_{22} & \hat{S}_{26} \\ \hat{S}_{16} & \hat{S}_{26} & \hat{S}_{66} \end{bmatrix}^{-1} = \hat{\mathbf{C}}_{TT} - \hat{\mathbf{C}}_{TN}\hat{\mathbf{C}}_{NN}^{-1}\hat{\mathbf{C}}_{NT} \quad . \qquad (13)$$

This is the general case of an anisotropic medium stiffened by arbitrarily anisotropic infinitely thin stiffening layers, or 'stiffeners'. The underlying stability of the material of the stiffeners (before $h \to 0$) implies that $\hat{\mathbf{S}}_{TT}$ is positive definite. Note that since the effect of the stiffeners comes from the values of $\hat{\mathbf{S}}_{TT}$ and $\hat{\rho}$ only, the stiffeners are inherently up-down symmetric, i.e., if they are embedded in a monoclinic background parallel to the mirror plane of symmetry, the stiffened equivalent medium retains that symmetry.

As a further assumption, let the components of $\hat{\mathbf{S}}$ satisfy constraints that are compatible with transverse isotropy, i.e.,

$$\hat{S}_{16} = \hat{S}_{26} = 0 , \qquad \hat{S}_{22} = \hat{S}_{11} , \qquad \hat{S}_{12} = \hat{S}_{11} - \hat{S}_{66}/2 . \qquad (14)$$

In this case, positive definiteness of $\hat{\mathbf{S}}_{TT}$ implies (in addition to the positiveness of the diagonal elements) that $\hat{S}_{66} < 4\hat{S}_{11}$. Then, carrying out the inversion and defining $\hat{\mu} \equiv 1/\hat{S}_{66}$ the excess shear rigidity and $\hat{M} \equiv \hat{S}_{11}/\hat{S}_{66}(\hat{S}_{11} - \hat{S}_{66}/4)$ the excess normal rigidity due to the presence of the stiffeners, one can write,

$$\hat{\mathbf{S}}_{TT}^{-1} = \begin{bmatrix} \hat{S}_{11}/\hat{S}_{66}(\hat{S}_{11} - \hat{S}_{66}/4) & \{\hat{S}_{66}/2 - \hat{S}_{11}\}/\hat{S}_{66}(\hat{S}_{11} - \hat{S}_{66}/4) & 0 \\ \{\hat{S}_{66}/2 - \hat{S}_{11}\}/\hat{S}_{66}(\hat{S}_{11} - \hat{S}_{66}/4) & \hat{S}_{11}/\hat{S}_{66}(\hat{S}_{11} - \hat{S}_{66}/4) & 0 \\ 0 & 0 & 1/\hat{S}_{66} \end{bmatrix}$$

$$= \begin{bmatrix} \hat{M} & \hat{M} - 2\hat{\mu} & 0 \\ \hat{M} - 2\hat{\mu} & \hat{M} & 0 \\ 0 & 0 & \hat{\mu} \end{bmatrix} , \qquad (15)$$

where

$$0 < \hat{\mu} < \hat{M} \quad .$$

Now, if the background is isotropic with Lamé parameters μ and λ, the 6×6 stiffness matrix of the stiffened medium is given by

$$\mathbf{c} = \begin{bmatrix} \lambda+2\mu+\hat{M} & \lambda+\hat{M}-2\hat{\mu} & \lambda & 0 & 0 & 0 \\ \lambda+\hat{M}-2\hat{\mu} & \lambda+2\mu+\hat{M} & \lambda & 0 & 0 & 0 \\ \lambda & \lambda & \lambda+2\mu & 0 & 0 & 0 \\ 0 & 0 & 0 & \mu & 0 & 0 \\ 0 & 0 & 0 & 0 & \mu & 0 \\ 0 & 0 & 0 & 0 & 0 & \mu+\hat{\mu} \end{bmatrix} , \qquad (16)$$

and clearly, since the stiffeners do not affect the isotropic values of c_{33}, c_{13} and c_{55}, the value of $c_{13} + 2\,c_{55} - c_{33} = 0$ (and $\Delta^T = 0$) as for isotropic media.

To form an ANNIE medium, one additional assumption is necessary, that $\hat{S}_{66}/\hat{S}_{11} = \hat{M}/\hat{\mu} = 2$. This condition is compatible with the stiffening material being isotropic with a dynamic Poisson's ratio equal to zero and its stiffness matrix is given by (16) with $\hat{M} = 2\hat{\mu}$. This is identical with the expression of (2) when μ_H is set equal to $\mu + \hat{\mu}$, so that $K_1 = \hat{\mu}/\mu$.

In contrast to ANNIE which is long wavelength equivalent to such plate stiffened media, one can define a class of TI media called K-media (Krey and Helbig, 1956) which are long wavelength equivalent to sets of constant γ isotropic layers. Making such a calculation yields a three-parameter TI medium with c_{55}/c_{33} equal to the chosen value of γ which also satisfies the constraint $c_{13} + 2c_{55} - c_{33} = 0$. However, instead of satisfying the additional simple ANNIE constraint that $c_{12} = c_{13}$, the additional constraint satisfied by K-media is that

$$c_{12} = c_{13}(c_{11} + c_{13})/(c_{33} + c_{13}) \quad . \qquad (17)$$

Since qP-wave behavior depends only on c_{11}, c_{33}, c_{55} and c_{13}, one can find a K-medium which has the same qP-wave slowness relation as an ANNIE medium. But from the physical interpretation, it may be seen that once shear is included, ANNIE is more suitable as a first cut for shales, whereas a K-medium would be better suited for modeling a sequence of fine layers whose compressional speed to shear speed ratio is approximately constant.

DISCUSSION AND CONCLUSION

A simple 3-parameter TI model has been presented. We propose that the behavior of this model may be used as a reasonable first approximation for the behavior of a wide variety of shales in the absence of further information on the behavior of a particular shale region. This model has the property that $c_{13} + 2\,c_{55} - c_{33} = 0$, and this condition allows the off-axis slowness to be predicted from measurements of propagation along the symmetry axis. This condition is consistent with the finding that reservoir depths obtained using P-wave stacking velocities are usually within 10% of actual depths (Winterstein, 1986).

Surface seismic exploration data is largely limited to compressional waves recorded in rather narrow aperture. Under these conditions a TI medium will "look isotropic" if the qP-wave move-out velocity is equal to the vertical P-wave velocity. A further constraint that $c_{12} = c_{13} \equiv \lambda$, often approximately satisfied, reduces the number of independent elastic parameters to three, and is consistent with the anisotropy being due solely to there being two shear moduli in the medium, the vertical shear modulus, $c_{55} \equiv \mu$, and the horizontal shear modulus, $c_{66} \equiv \mu_H \neq \mu$. The positive anellipticity characteristic of shales follows if μ_H is greater than μ. Because qP-waves are of paramount importance, we have presented a simple and accurate approximate qP slowness relation for ANNIE media in terms of zero-offset normal moveout velocity α and the horizontal velocity, α_H given by (8). This is by no means the only such approximation possible (see, for example, Muir's anelliptic approximation (Dellinger et al., 1993), or the approximation obtained from taking the limit of the exact slowness relation (7) and letting $\beta \to 0$). However, the approximation given here is easy to interpret and trivial to implement numerically in that the normalized vertical slowness squared $\alpha^2 p_z^2$ is given as a product of $1 - \alpha_H^2 p_x^2$, an elliptical anisotropy term linear in horizontal slowness squared, and $1 + \Delta\alpha_H^2 p_x^2$, a term, also linear in horizontal slowness squared, which accounts for the anellipticity while forcing the curvature of the slowness curve at the vertical axis to be $-\sqrt{\alpha}$, i.e., what it would be if the medium were isotropic.

We have also demonstrated that there is a physical interpretation for an ANNIE medium; an ANNIE medium is long wavelength equivalent to an isotropic medium stiffened by thin rigid parallel plates, in the limit as the stiffeners become infinitely thin while becoming infinitely rigid. It is suggestive that shales are composed largely of relatively hard platelets which are roughly aligned normal to the TI symmetry axis.

ACKNOWLEDGEMENT

We would like to acknowledge the contribution of Professor Adnan Nayfeh of the University of Cincinnati. The formulation of the properties of thin plate stiffened media was developed jointly by one of the authors (MS) and Professor Nayfeh through a series of discussions several years ago. We also want to express our appreciation to John Cook of Schlumberger Cambridge Research for the use of the very illustrative scanning electron microscope shale photograph, Fig. 1.

REFERENCES

Carrion, P., Costa, J., Ferrer Pinheiro, J.E. and Schoenberg, M., 1992. Cross-borehole tomography in anisotropic media. Geophysics, 57: 1194-1198.

Dellinger, J., Muir, F. and Karrenbach, M., 1993. Anelliptic approximations for TI media. Jrnl. of Seismic Explor., 2: 23-40.

Hornby, B.E., 1994. The Elastic Properties of Shales. PhD thesis, University of Cambridge, Cambridge, U.K.

Hornby B.E., Schwartz, L.M. and Hudson, J.A., 1994. Anisotropic effective medium modeling of the elastic properties of shales. Geophysics, 59: 1570-1583.

Johnston, J.E. and Christensen, N.I., 1995. Seismic anisotropy of shales. J. Geophys. Res. B, 100: 5991-6003.

Jones, L.E.A. and Wang, H.F., 1981. Ultrasonic velocities in Cretaceous shales from the Williston basin. Geophysics, 46: 288-297.

Krey, Th. and Helbig, K., 1956. A theorem concerning anisotropy of stratified media and its significance for reflection seismics. Geophys. Prosp., 4: 294-392.

Sayers, C.M., 1994. The elastic anisotropy of shales. J. Geophys. Res. B, 99: 767-774.

Schoenberg, M., 1994. Transversely isotropic media equivalent to thin isotropic layers. Geophys. Prosp., 42: 885-915.

Schoenberg, M. and Douma, J., 1988. Elastic wave propagation in media with parallel fractures and aligned cracks. Geophys. Prosp., 36: 571-590.

Schoenberg, M. and Muir, F., 1989. A calculus for finely layered anisotropic media. Geophysics, 54: 581-589.

Swan, G., Cook, J., Bruce, S. and Meehan, R., 1989. Strain rate effects in Kimmeridge Bay shale. Int. J. Rock Mech., 26: 135-149.

Thomsen, L., 1986. Weak elastic anisotropy. Geophysics, 51: 1954-1966.

Vernik, L. and Nur, A., 1992. Ultrasonic velocity and anisotropy of hydrocarbon source rocks. Geophysics, 57: 727-735.

Winterstein, D.F., 1986. Anisotropy effects in P-wave and SH-wave stacking velocities contain information on lithology. Geophysics, 51: 661-672.